Designing of Cascade Controller by Using the Bees Algorithm

MURAT SAHIN*
Control Systems Department
Roketsan Inc.
Ankara, TURKEY

GOKSEL KIZIR
Control Systems Department
Roketsan Inc.
Ankara, TURKEY

Abstract: - In this study, studies were carried out within the scope of the control of high-speed mini direct current (DC) motor. A cascaded controller with position, speed, and current control has been developed to precisely and robustly control the DC motor. While optimizing the controller parameters, a multi-objective Bees Algorithm (BA) was used to minimize settling time, rise time, overshoot, and system error. As a result of simulations, low settling and rise times with multi-objective BA were achieved, while overshoot was also not allowed. Also, verification of the controller was carried out with experimental studies. Experimental results and simulation results overlap with less than a 1% difference.

Key-Words: - The Bees Algorithm, Optimization, DC motor, Cascade controller, PID control, Design
Received: May 15, 2022. Revised: September 13, 2022. Accepted: October 11, 2022. Published: November 17, 2022.

1 Introduction

DC motor is used in many different areas because of their low maintenance cost, the volume of sufficient torque, high speed, and high reliability, [1]. Because of these specifications, it is considered by some researchers to be the ideal DC motor for aerospace applications, [2]. It is used with the gearbox in the case of higher torque requirements, such as the control of aircraft wings, [3]. Electromechanical actuators are one of the critical systems in aviation. Of course, new developments in DC motor technologies, which are their main components, also play an active role in this case, [4]. The control process can be complex, especially in DC motors with low resistance and high speed. More robust controllers can be obtained in DC motor speed control by using the current sensor in combination with the current control, [5, 6]. Although different types of control systems have been developed over the years, PID controllers are still at the forefront of DC motor control. Especially with the development of adaptive and robust PIDs, improved PID algorithms have become popular again. The critical stage of PID control is setting parameters. In this context, Root Locus (RL) analyses have been used for years and verified in many industrial applications, [7].

Although RL analysis gives good results in industrial applications, different methods may be required in highly dynamic systems such as aviation and aerospace. Population-based algorithms are frequently used in tuning for these parameters of control systems. Control systems have multiple objects that need improvement, such as rising time, settling time, overshoot, and controller error. These optimization problems are multi-objective (MO) optimization problems. In some systems, these functions may act opposite one another. Therefore, while one increases, the other may decrease, [8]. In this case, one of the most preferred methods is the Weighted Sum Method. Here, all objective has a weighting factor, and multiple solutions are combined into one solution, [9, 10]. It is seen in the literature that population-based algorithms for MO function problems give good results. The PID parameters of the velocity control were tuned with the ACO, [11]. In another study [12], MO-PSO was tried to obtain a more robust PID control. In another study [13], the parameters of the PID used to control the automatic voltage regulator system were tuned with MO-PSO. One of the other popular algorithms is the bees algorithm (BA) developed by Pham et al. , [14]. Although it is frequently used in optimizing different problems, it has only been used a little in control applications for many years. In one of the first applications, Coban and Ercin [15] optimized the parameters of PID control with the MO-BA within the scope of the speed control of the DC motor. It was used by Shouran et al. in 2021 to optimize PID and sliding mode control parameters, [16, 17]. In another study in the same year, Esleman et al. used it for PID and fuzzy logic controller optimization, [18]. It was also used for sliding mode control by İlgen et al. in 2022, [19].

From the studies given above, it is seen that BA gives successful results within the scope of optimization of different control systems. In this study, a cascade PID control system has been developed to control DC motor dynamics more precisely. The DC motor model and controller structure are shown in the second part of this study. The parameters of each control loop were adjusted with multi-objective BA, and in the third part, these studies are shown. After that, experimental studies were done for multi-objective BA parameters. There are experimental results and comparisons with simulation in the last section.

2 DC Motor Model and Cascade Control

Electrical (1) and mechanical equations (2) and (3) of the DC motor are shown, [20].

$$V = \frac{di}{dt}L + Ri + \omega K_b \quad (1)$$

$$T = \frac{d\omega}{dt}J + \omega B + T_L \quad (2)$$

$$T = iK_t \quad (3)$$

The V, T, and TL parameters used in Equations (1), (2), and (3) represent motor voltage, motor electrical torque, and load torque, respectively. (The parameters of the DC motor are given in Appendix.)

2.1 The Structure of Cascade Control

Cascade controllers have multiple nested control systems. The output of the first controller is used as input to the second controller. Likewise, the output of the second becomes the input of the third. Each control loop must have its feedback. Therefore, the cascade control system is only suitable for systems with many sensors, [21]. In this study, a three-loop cascade control system was designed. The inner loop is current control, the second loop is velocity control, and the outer loop is position control. The cascade control structure is presented in Figure 1.

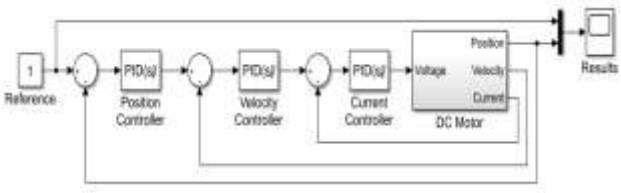

Figure 1. The Structure of Cascade Control

In the cascade controller, the loops should be designed as outer loops from the inner loop. In addition, each loop should be designed to be at least 4-5 times faster than an outer loop so that the dynamics of these loops do not affect each other, [22]. As the design criterion, the bandwidth of the position loop was determined in the range of 20-25 Hz. In order to determine the controller parameters, it is also necessary to define the steady-state errors and maximum overshoot limits. Within the scope of the study, the requirements determined for each loop are presented in Table 1.

Table 1. Requirements of Controller Loops

Controller Requirements	*Controller*		
	Current Loop	*Velocity Loop*	*Position Loop*
Bandwidth (Hz)	600 - 650	140 - 160	20 - 25
Steady State Error (%)	≤ 10	≤ 5	≤ 0
Max. Overshoot (%)	≤ 10	≤ 5	≤ 0

3 Designing Cascade Controller by Using the Multi-Objective BA

The foraging strategy of honey bees inspires BA. The scout bees communicate with other bees in the hive with a special dance (weggle dance). Because of this communication, most worker bees are directed to the most productive areas. This situation inspired the local search section of the algorithm. On the other hand, scout bees continue to search for more productive areas. This section inspired the global search section. This way, optimum global values are reached without getting stuck with local optimum values, [14, 23].

Population size (Scout bees) is one of the critical parameters in BA. The population size (n) is usually between 30 and 100. This study was set as 30 to shorten the optimization time. The local search sites (Selected site, m) were determined to be 30% of the population. The elite sites (e) were determined as 30% of the selected sites. The algorithm parameters used in this study are given in Table 2. The neighborhood parameter is an essential concept for all evolutionary algorithms. This algorithm adjusts the neighborhood size to get smaller at each iteration. This way, neighbors of good sites are sought more, [24].

Table 2. Parameters of BA

Parameters	*Value*
Number of iterations	30
Number of scout bees (n)	30
Number of bees for elite sites (nep)	30
Number of bees for selected sites (nsp)	10
Number of elite sites (e)	3

Number of selected sites (m)	9

3.1. Multi-Objective Optimization

MO optimization aims to show the trade-offs between objectives and give the designer a general view of the problem. MO optimization also tries to minimize all objective functions. The general definition is given in (4), [25].

$$Min\ f(x) = (f_1(x), f_2(x), \dots, f_m(x)) \qquad (4)$$

In this study, the weighted sum method was used. The integral of the square of the error (ISE), maximum percent overshoot (MPO), rise time (RT), and settling time (ST) have been determined as objective functions. All components are required to be minimum. The multi-objective function used in the algorithm is given below.

$$MOF = \lambda_1 ISE + \lambda_2 RT + \lambda_3 ST + \lambda_4 MPO \qquad (5)$$

It is seen in (5) that a single function is created from the sum of all the objectives. The critical issue here is to define lambdas. There are different methods in the literature, and these are generally fixed values. Fixed coefficients may differ from system to system. In order to find fixed lambdas for any system, it is necessary to verify by doing many tests. Therefore, constant lambda values were not used in this study. Lambdas are determined interactively within BA. While the controller parameters that will make the MOF minimum in each cycle are determined, lambda is determined by bee dance similarly. In this way, while the minimum MOF value is found in each iteration, because of the variable lambda values, different value ranges of the objectives can be seen. So, the most suitable solution can be determined according to the requirements. Alternatives can be determined where ISE is minimum, RT and ST are medium, or all are between minimum and medium. The local search section of MO-BA is given in Figure 2.

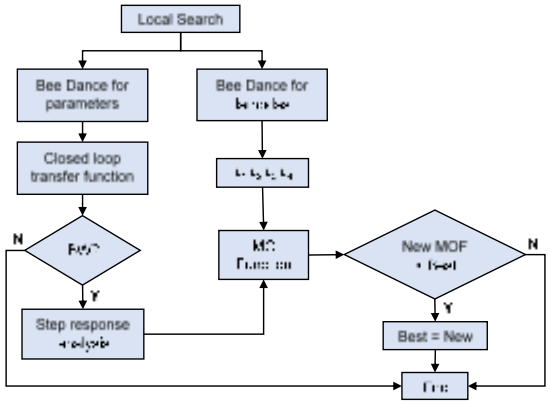

Figure 2. The flowchart of the local search section

3.2. Current Controller

The current loop calculates the voltage value required to perform the current command to the DC motor. The transfer function between the voltage applied to the DC motor, and the current form is given in Equation (6), [20].

$$TF_C = \frac{Js+B}{JLs^2+(BL+JR)s+(BR+K_bK_t)} \qquad (6)$$

The current loop should limit these high currents and ensure that its current increase in a controlled manner. In order to reduce the steady-state error in the current loop, a PI controller should be used, [22]. It is shown in Figure 3 by tuning the parameters of the current controller with the MO-BA. Ranges of lambda values were chosen between 0 and 1 in the bee's dance.

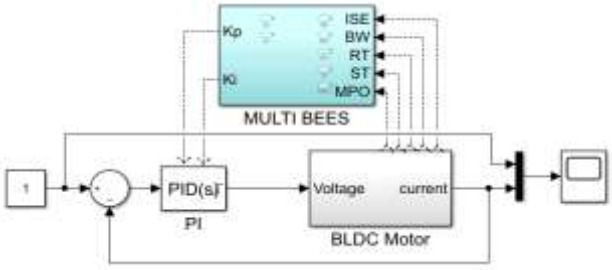

Figure 3. Model of current controller's parameters tuning with MO-BA

While evaluating the results in Figure 6, the section where MOF is minimum is checked first. This area is also where ISE, RT, and ST are minimum. (The MPO value is not shown in the graph because it is 0.) Therefore, for the current controller parameters, the last step of the iteration is evaluated.

3.3. Velocity Controller

The velocity loop must calculate the current applied to the motor to perform the velocity command. In this context, it is necessary to calculate the transfer function between the current reference and the motor angular velocity. At the same time, the current controller calculated above is added. Again, to reduce the steady-state error, a PI controller was used, [22]. The velocity loop block diagram (TF_w) is shown in Figure 4.

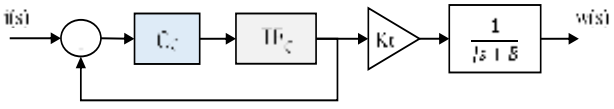

Figure 4. Velocity Loop Block Diagram

3.4. Position Controller

The position loop must calculate the velocity value applied to the motor to perform the position command. The position loop block diagram is shown in Figure 5. The velocity controller above was also added. There is a free s term in the position loop transfer function. So, there will be no steady-state error in the closed-loop system. Therefore, control loop requirements can be met with the P controller.

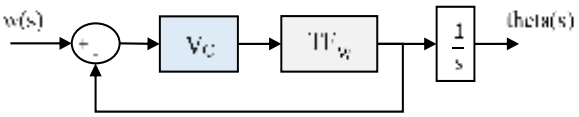

Figure 5. Position - Open Loop Transfer Function

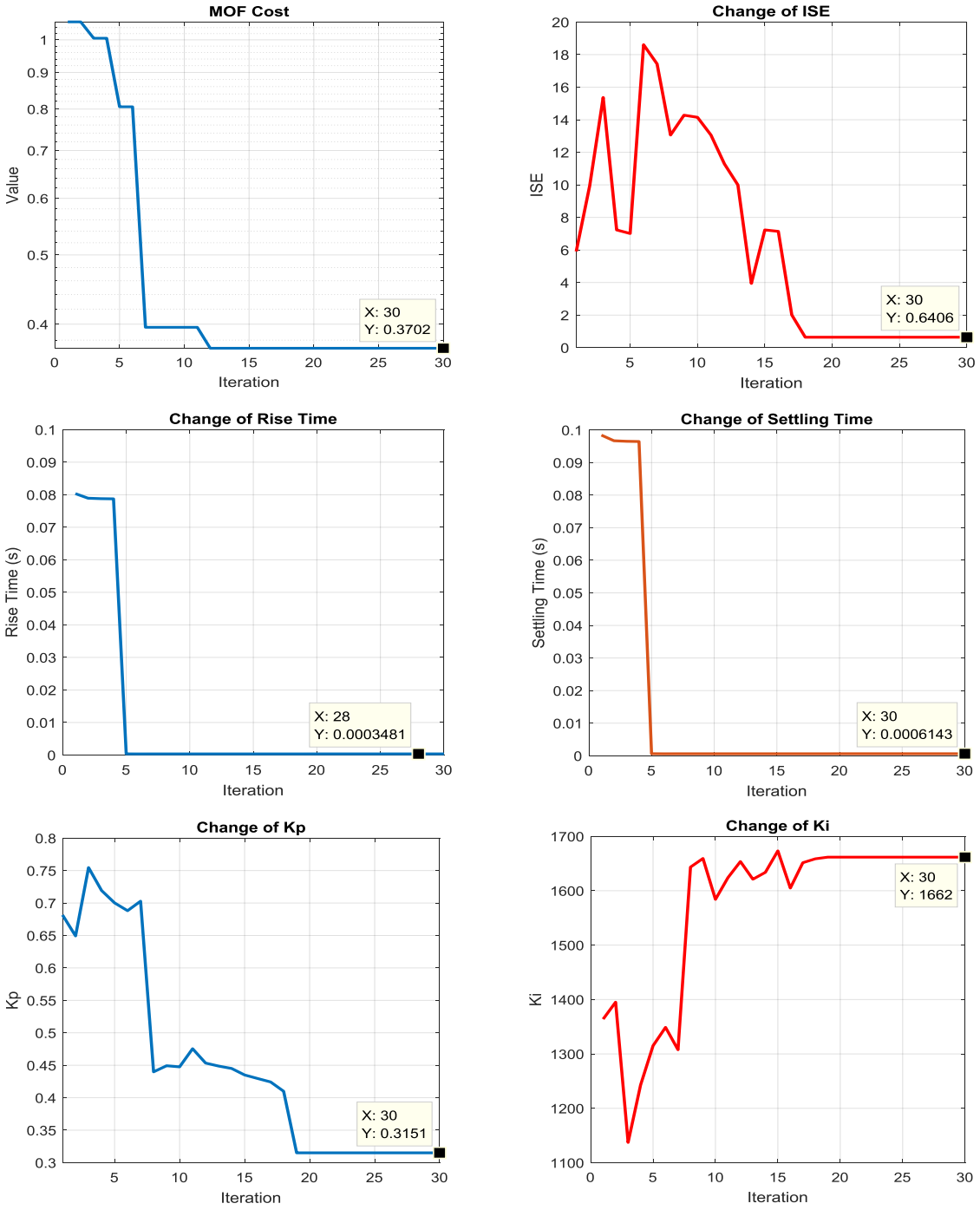

Figure 6. MOF cost, ISE, rise time, settling time, Kp, and Ki of the current controller

4 Experimental Studies and Analyses

4.1. Simulation Results

First, simulations are made in Matlab to calculate the coefficients of each controller. In order to see the repeatability of the optimization algorithm, ten consecutive tests were carried out. All optimization results are given in Table 3.

Table 3. Optimization Results

Sim.	Cur. Cont.		Vel. Cont.		Pos. C.
	P	I	P	I	P
1	0.2933	1588	0.1241	0.00044	103.3
2	0.2912	1602	0.1194	0.00029	107.6
3	0.2722	1541	0.1156	0.00097	111.6
4	0.3151	1662	0.1175	0.00068	112.3
5	0.3015	1598	0.1194	0.00049	104.3
6	0.3116	1605	0.1242	0.00093	102.9
7	0.3287	1677	0.1218	0.00028	104.1
8	0.2945	1580	0.1236	0.00054	111.6
9	0.3136	1610	0.1248	0.00097	103.9
10	0.3127	1626	0.1191	0.00019	111.6

In order to test the coefficients, a one-rad/s step command was first applied to the velocity control loop. The results of the simulations using the coefficients in Table 3 are shown in Figure 7 and 8.

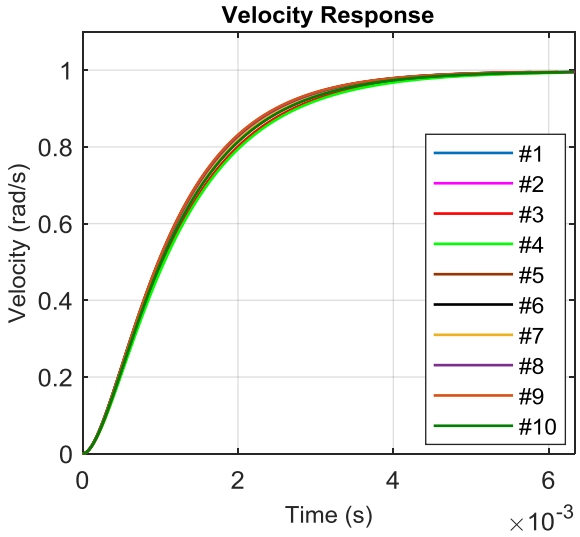

Figure 7. Step response of the velocity control

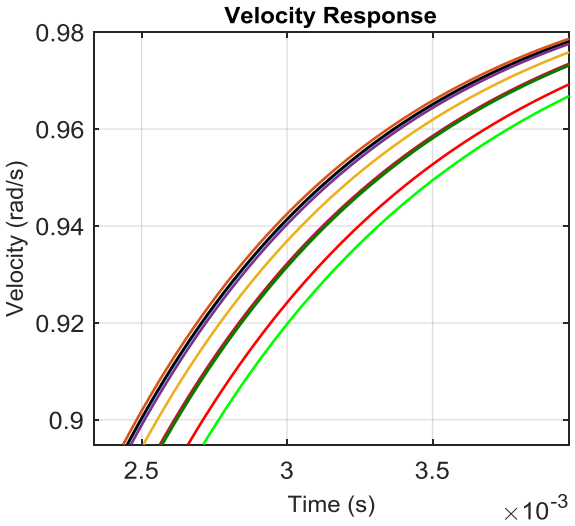

Figure 8. Step response of the velocity control (zoom)

It is seen that MO-BA has no MPO and no steady-state error. In this simulation, the rise times are 2.2 – 2.4 ms, and the settling times are between 4 - 4.6 ms. Bode diagrams were also preferred within the scope of bandwidth control, [26]. Bandwidth values of all simulations were found in the range of 140 to 160 Hz, following the requirements. The Bode diagram is given in the Appendix (Figure 26). At last, the one rad step command was applied to the position control loop. The results are given in Figure 9 and Figure 10.

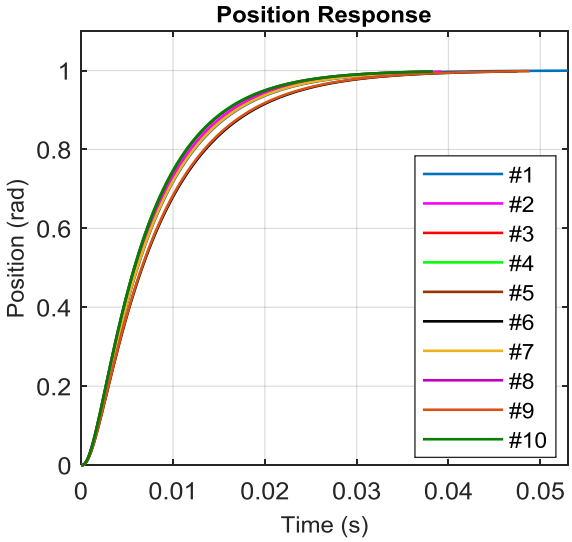

Figure 9. Step response of the position control

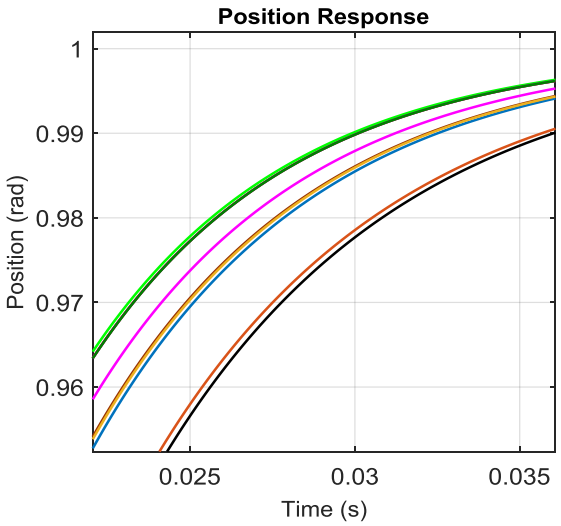

Figure 10. Step response of the position control (zoom)

As in velocity control, control can be provided without overshoot and steady-state error in position control. In these simulations, the rise times are between 14 - 15 ms, and the settling times are between 26 - 30 ms. 9A (Peak current, Figure 11) was drawn from the motor during the movement. The peak current of the motor is above 100A, so it has been seen that the current loop works successfully and limits the current during the position control. Bandwidth values of all simulations were found in the range of 20 to 25 Hz, following the requirements. The Bode diagram is given in the Appendix (Figure 27).

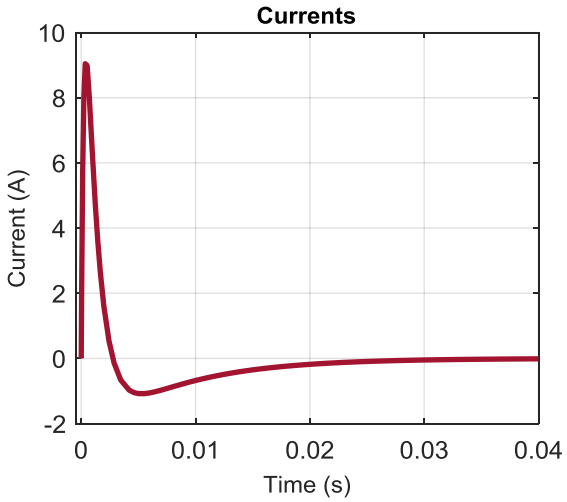

Figure 11. Current Data

Among the values in Table 3, the coefficients in the 4th line, which have the fastest settling time value in the position control, were selected. The PI controller obtained for the current loop is given in equation (7), and the controller for the velocity loop is given in equation (8). The P controller for the position loop is given in equation (9).

$$C_C = 0.3151 + \frac{1662}{s} \tag{7}$$

$$V_C = 0.1175 + \frac{0.00068}{s} \tag{8}$$

$$P_C = 112.3 \tag{9}$$

4.2. Experimental Results

The microcontroller-based driver circuit is used for both DC drive and cascade control. The driver card and other equipment used in the experiments can be seen in Figure 12.

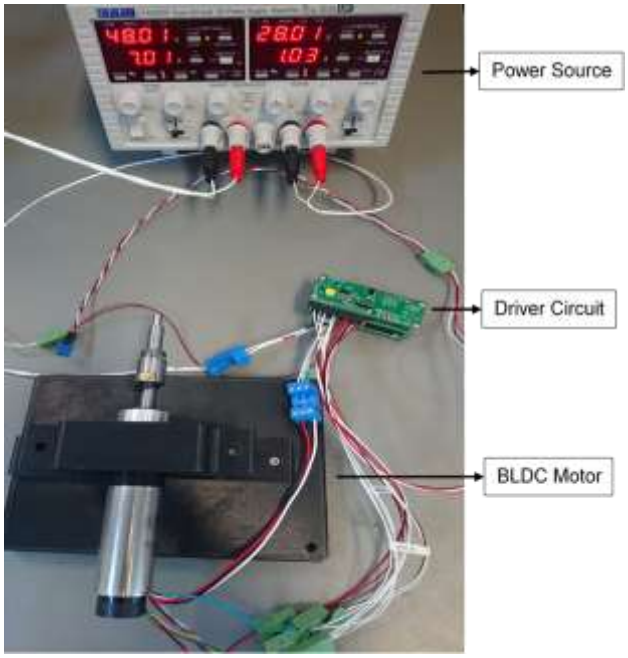

Figure 12. Experimental environment

First, a 1-degree step command was applied and compared with simulation results. The results are shown in Figure 13 and Figure 14. As can be seen, experimental results and simulation results overlap. Figure 15 shows the effect of the digital controller at only 1x10-3 degrees.

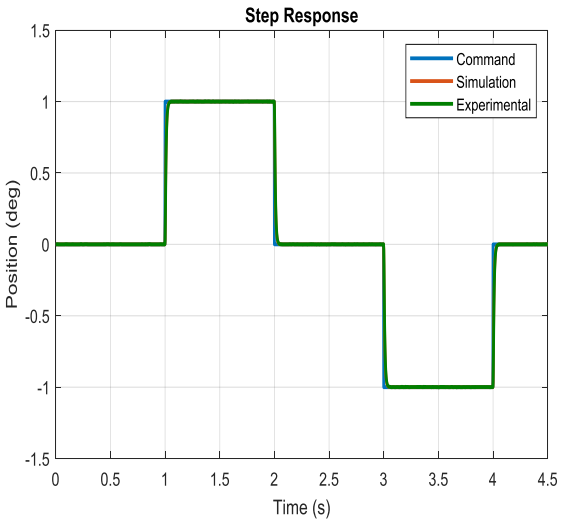

Figure 13. Experimental results of position control

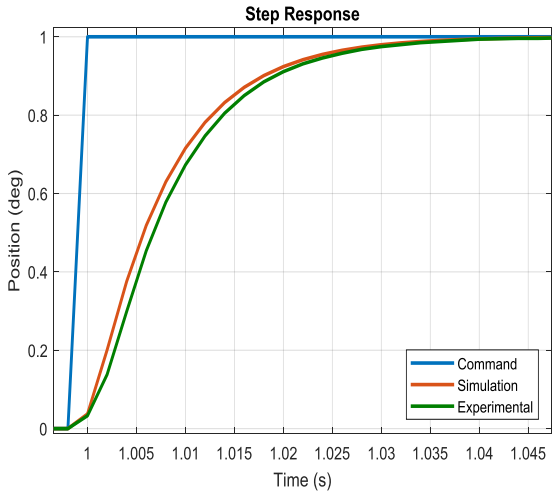

Figure 14. Zoomed view of results - 1

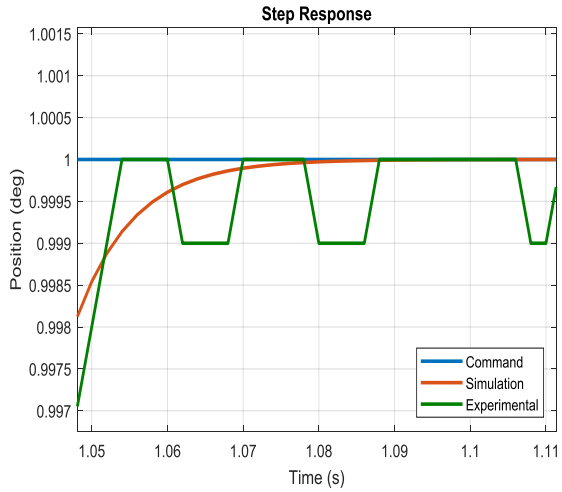

Figure 15. Zoomed view of results – 2

The currents of the DC motor are shown in Figure 16. Actual currents and simulation data overlap. Noise is observed in experimental studies. This noise difference is expected because the equipment, the sensor, and the driver were not modeled in the simulation.

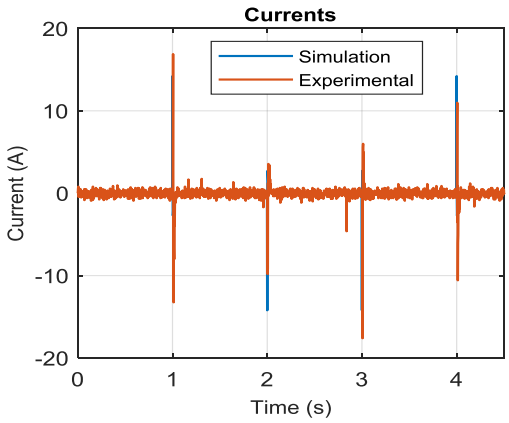

Figure 16. Experimental results of current data

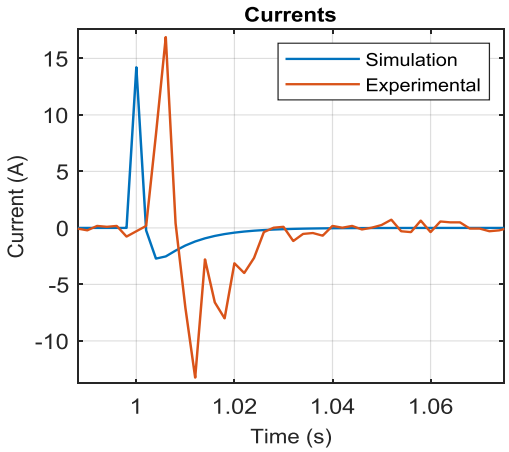

Figure 17. Zoomed view of these results

The bandwidth test was the second test to verify the cascade controller. For this purpose, a chirp signal (From 1 to 25 Hz, increasing 1Hz at 1-second steps.) was applied to the DC motor. Test results and comparison with simulation are given in Figures 18 and 19.

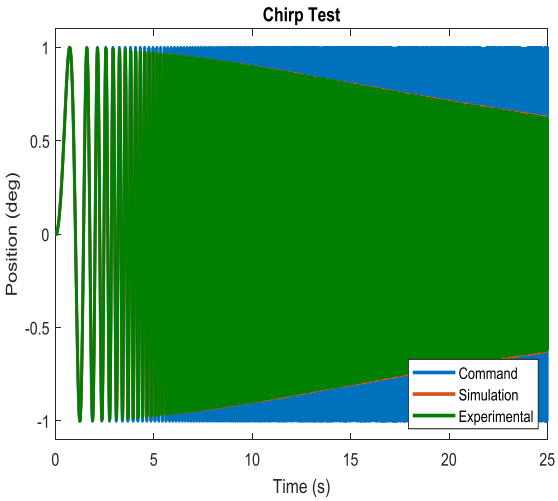

Figure 18. Experimental results of bandwidth test

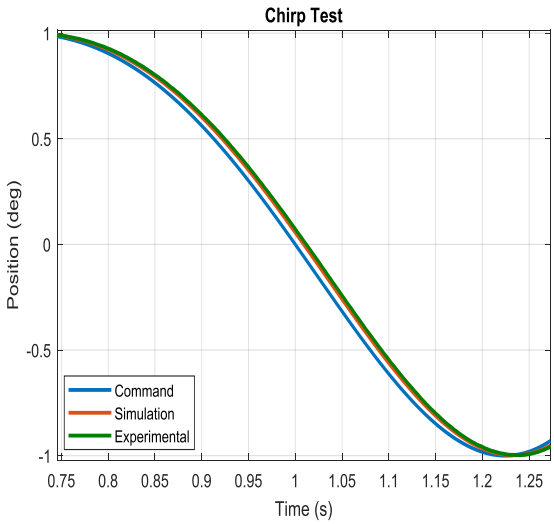

Figure 19. Zoomed view of these results - 1

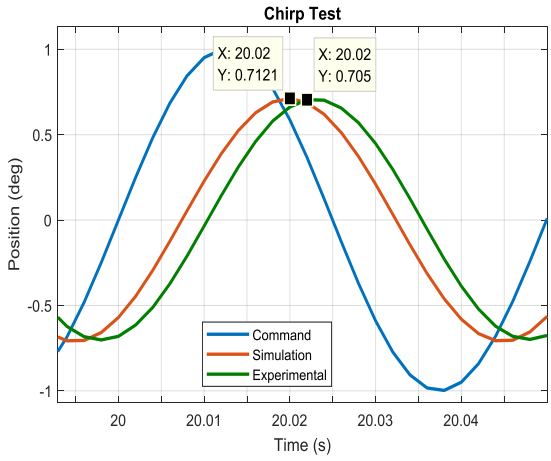

Figure 20. Zoomed view of these results – 2

As can be seen from the figures, the DC motor can respond to the command of 20 Hz with the cascade controller. These results also overlap with simulation results. There is very little difference due to hardware effects.

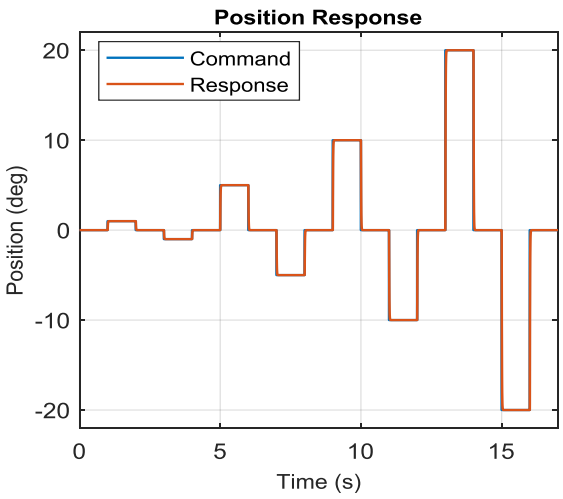

Figure 21. Responses to high amplitude commands

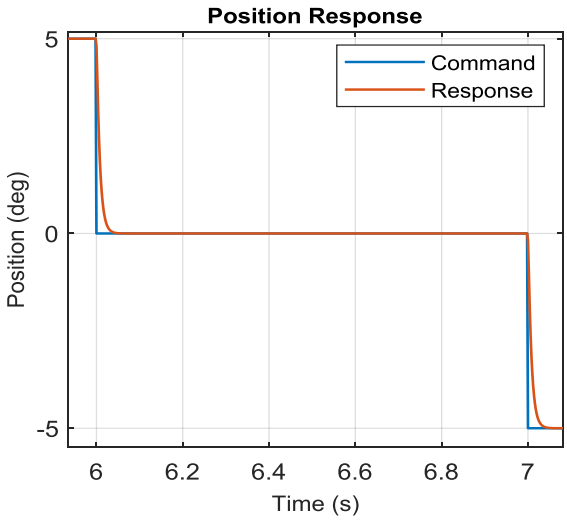

Figure 22. Responses to high amplitude commands (zoom)

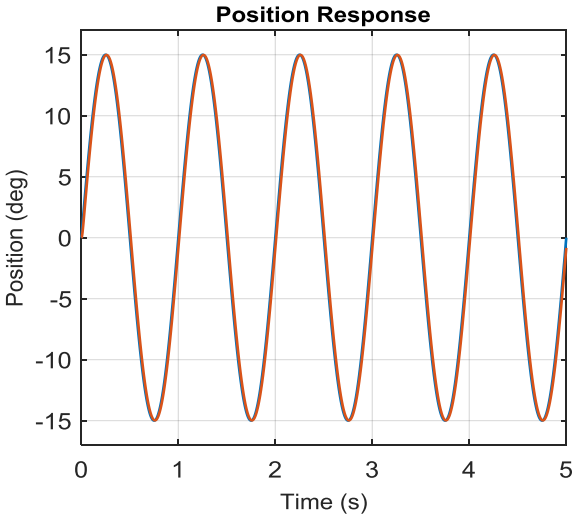

Figure 23. Responses to high amplitude sine commands

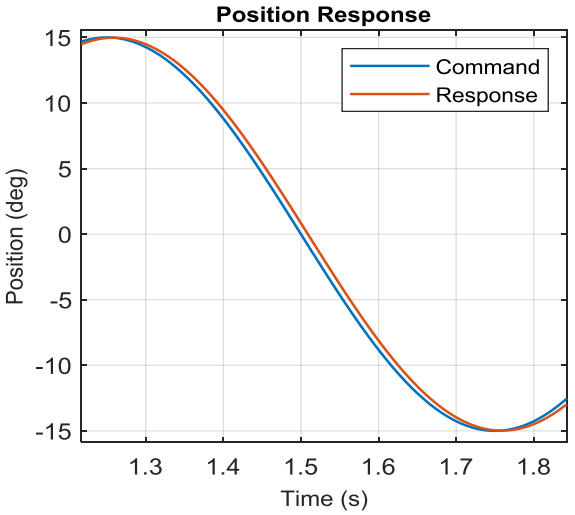

Figure 24. Responses to high amplitude sine commands (zoom)

Finally, high amplitude step and sine commands were applied to test the controllers, and conditions such as steady-state error and overshoot were observed. Test results are given in Figures 20 – 23. As can be seen from the results, the designed controllers could respond to step and sinus commands of 15-20 degrees without overshoot and steady-state error.

When controlling the DC motor at high speed, overshoot can be expected. Moreover, these overshoots cause momentary high currents to be created from the motor. As can be seen in the results above, there was no overshoot because four different parameters were controlled at the same time.

4 Conclusion

In this study, the position control of a mini high-speed DC motor was performed. The cascade controller is designed to achieve better energy efficiency and more precise and robust control. BA, a population-based search, and an optimization method were used to adjust the parameters of the cascade controller. Because the control system has more than one part of being minimized, a multi-objective BA has also been designed. All parameters were compared by testing both in simulation and experimental environments. With MO-BA, in which the error, settling time, rise time, and overshoot are controlled together, it is seen that effective control can be done. MO-BA achieved lower settling and rise times in each control loop without overshoot. In order to verify the MO-BA, a test environment was prepared. Firstly, the position control was made with the step command, and it was seen that the results matched precisely with the simulation. In position tracking, there are differences in mili radian levels due to hardware factors. In the second test, in order to verify the bandwidth, a constant amplitude sine signal was applied with increasing frequency over time. With this test, the 20 Hz bandwidth obtained in simulations was verified in the experimental environment. As a result of the studies, it has been observed that the Multi-Objective Bees Algorithm successfully tunes the parameters of cascade PID controllers used extensively in different fields. It is evaluated that this algorithm can be applied to different systems and different controllers by updating.

No external load was used in the studies. In future studies, tests can be repeated using external dynamic loads, and optimization studies can be updated if necessary. In addition, online optimization is planned as another future work.

Competing interests

The authors declare that they have no competing interests.

REFERENCES

[1]. Colak, I., Sahin, M., Esen, Z., Artificial neural networks controller algorithm developed for a brushless DC motor, IEEE 12th International Conference on Machine Learning and Applications, 2013, 238-242.

[2]. Praveen, R.P., Ravichandran, M.H., Sadasivan Achari, V.T., Jagathy Raj, V.P., Madhu, G., Bindu, G.R., and Dubas, F., Optimal design of a surface-mounted permanent-magnet BLDC motor for spacecraft applications, International Conference on Emerging Trends in Electrical and Computer Technology, 2011, 413-419.

[3]. Peng, Y., Liu, L., Zhang, Y., Cao, J., Cheng, Y., Wang, J., A smooth impact drive mechanism actuation method for flapping-wing mechanism of bio‐inspired micro air vehicles, Microsyst Technol, 2018, 24, 935–941.

[4]. Zhang, J., Zhou, J., Design, and optimization of an adjustable electromechanical actuator, IEEE Information Technology and Mechatronics Engineering Conference (ITOEC), 2017, 272-275.

[5]. Efe Kayabaşı, S., Erzan Topçu, E., Investigation the Effect of Design Parameters of Miniature Brushless DC Motors Used in Industrial Applications, ElCezerî Journal of Science and Engineering, 2019, 6(2), 236-250.

[6]. Şimşek, E. C., Köse, A., Şahin, M., & Irmak, E. (2019, November). Optimization of PID parameters using ant colony algorithm for position control of DC motor. In 2019 8th International Conference on Renewable Energy Research and Applications (ICRERA) (pp. 1047-1051). IEEE.

[7]. Yuce, A., Tan, N., Dogruer, T., Root-locus analysis of fractional-order transfer functions using LabVIEW: An interactive application, 6th International Conference on Control Engineering and Information Technologies, 2018, 245-250.

[8]. Etesami, G., Felezi, M. E., Zadeh, N. N., Pareto optimal multi-objective dynamical balancing of a slider-crank mechanism using differential evolution algorithm, International Journal of Automotive Engineering, 2019, (9)3:3021-3032.

[9]. Gunantara, N., A review of multi-objective optimization: Methods and its applications, Journal Cogent Engineering, 2018, (5)1:1-16.

[10]. Sahin, M., Optimization of Model Predictive Control Weights for Control of Permanent Magnet Synchronous Motor by Using the Multi-Objective Bees Algorithm. Model-Based Control Engineering - Recent Design and Implementations for Varied Applications [Working Title], edited by Umar Hamid, Ahmad Faudzi, IntechOpen, 2021, 1-20.

[11]. Navidi, N., Bavafa, M., Hesami, S., A new approach for designing of PID controller for a linear brushless dc motor with using ant colony search algorithm, Asia-Pacific Power and Energy Engineering Conference, 2009, 1-5.

[12]. Zhao, S. Z., Iruthayarajan, M. W., Baskar, S., Suganthan, P.N., Multi-objective robust PID controller tuning using two lbests multi-objective particle swarm optimization, Information Sciences, 2011, 181, 3323–3335.

[13]. Sahib, M. A., Ahmed, B. S. A new multiobjective performance criterion used in PID tuning optimization algorithms, Journal of Advanced Research, 2016, 7, 125–134.

[14]. Suliman, F., Anayi, F., & Packianather, M. Bees-Algorithm for parameters identification of PV Models. IEEE 2nd International Conference on Advance Computing and Innovative Technologies in Engineering (ICACITE), 2022, pp. 2219-2223.

[15]. Coban, R., Ercin, O., Multi-objective bees algorithm to optimal tuning of PID controller, Çukurova University Journal of the Faculty of Engineering and Architecture, 2012, 27(2), 13-26.

[16]. Shouran, M., Anayi, F., & Packianather, M., The Bees Algorithm Tuned Sliding Mode Control for Load Frequency Control in Two-Area Power System, Energies, 2021, 14(18), 5701.

[17]. Shouran, M., Anayi, F., Packianather, M., & Habil, M., Load frequency control based on the bees algorithm for the great britain power system, Designs, 2021, 5(3), 50.

[18]. Esleman, E. A., Önal, G., & Kalyoncu, M., Optimal PID and fuzzy logic based position controller design of an overhead crane using the Bees Algorithm, SN Applied Sciences, 2021, 3(10), 1-13.

[19]. İlgen, S., Durdu, A., Gülbahçe, E., Çakan, A., & Kalyoncu, M., The Bees Algorithm Approach to Determining SMC Controller Parameters for the Position Control of a SCARA Robot Manipulator, Avrupa Bilim ve Teknoloji Dergisi, 2022, (33), 267-273.

[20]. Karapinar, U., Esen, Z., Sahin, M., Kanburoglu, F., Cascaded controller algorithm design for a brushless DC motor with Matlab/Simulink and MCU implementation, 21st Signal Processing and Communications Applications Conference (SIU), 2013, 1-8.

[21]. Bolton, W., Instrumentation, and control systems, Second Edition, Elsevier Ltd., 2015, 290-302.

[22]. Ogata, K., Modern control engineering, Prentice Hall, 4th Edition, 2002, 492-499.

[23]. Bahari, M. S., Azmi, N. A., Yusof, Z. M., & Pham, D. T., Bees Algorithm with Integration of Probabilistic Models for Global Optimization, In Intelligent Manufacturing and Mechatronics, 2021, 269-277.

[24]. Baronti, L., Castellani, M., & Pham, D. T., An analysis of the search mechanisms of the bees algorithm, Swarm and Evolutionary Computation, 2020, 59, 100746.

[25]. Tian, Y., Si, L., Zhang, X., Cheng, R., He, C., Tan, K. C., & Jin, Y., Evolutionary large-scale multi-objective optimization: A survey, ACM Computing Surveys (CSUR), 2021, 54(8), 1-34.

[26]. Golnaraghi, F., Kuo, B. C., Automatic control systems, John Wiley & Sons. Inc., 9th Edition, 2009, 455-462.

Appendix 1 - DC Motor Parameters

Parameters	***Value***
Inductance (mH)	0.065
Resistance (ohm)	0.39
Power (w)	200
Supply voltage (V)	48
Inertia (kg.m^2)	33x10^{-7}
Back EMF (V/rad/s)	0.027
Torque constant (Nm/A)	0.027

Appendix 2 – Bode Diagrams

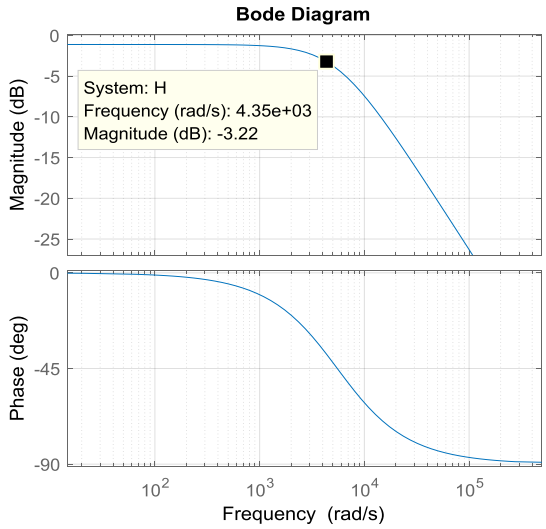

Figure 25. Bode diagram of current loop

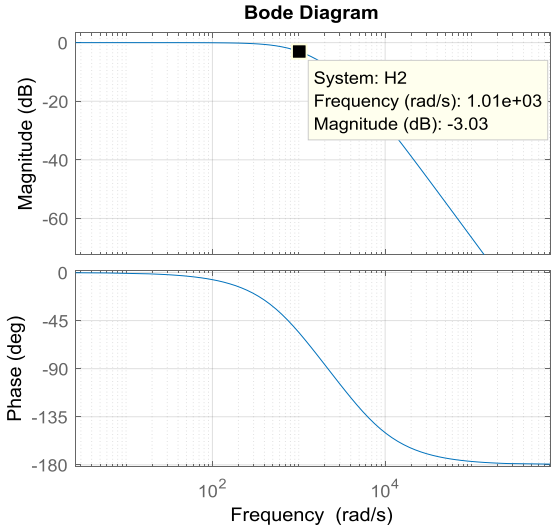

Figure 26. Bode diagram of velocity loop

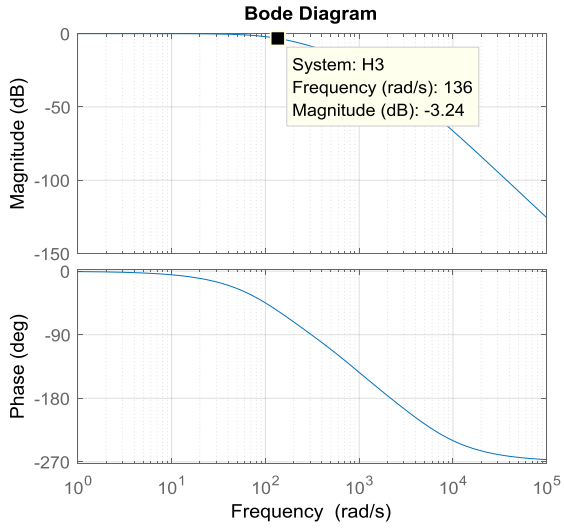

Figure 27. Bode diagram of position loop